Effects of higher-J states on nuclear-spin relaxation times for H_2 and D_2 in amorphous silicon

R. E. Norberg
Department of Physics, Washington University, St. Louis, Missouri 63130
(Received 9 October 1984)

Fedders' calculations of the effects of molecular $J > 1$ states on the nuclear-spin-lattice relaxation of H_2 and D_2 are applied to the interpretation of proton and deuteron relaxation in amorphous silicon. The temperature dependence of proton relaxation in three plasma-deposited a-Si:H samples indicates that the effectively dilute o-H_2 molecules controlling the relaxation occupy at least two different kinds of sites. Depending on sample preparation conditions, there are predominant o-H_2 sites with large static electric field gradients of different symmetries. Deuteron relaxation times in the a-Si:D,H sample cannot be fitted by the calculated temperature dependence of D_2-related relaxation. It is probable that motional narrowing reduces the effectiveness of the spin-diffusion contact between deuterons and D_2 relaxation centers above 40 K.

Recently Fedders has reported calculations[1] of the effect of molecular $J > 1$ states on nuclear-spin-lattice relaxation times for isolated H_2 or D_2 molecules in solid nonmagnetic hosts. The relaxation includes contributions from higher-J states to the nuclear relaxation of dilute o-H_2, p-D_2, and o-D_2 above 100 K. Strikingly different temperature variations are predicted for the warm-sample nuclear relaxations corresponding to three analyzed symmetries of large static electric-field gradients (EFG): no symmetry, axial symmetry, and cubic symmetry (that is, no EFG).

The present paper compares the calculated temperature dependences of nuclear relaxation times $T_1(H_2)$ and $T_1(D_2)$ to proton and deuteron spin-lattice relaxation times reported for H and D in some amorphous silicon samples at temperatures up to 600 K. Because of rapid spin diffusion, the $T_1(H)$ and $T_1(D)$ have temperature variations that follow those of $T_1(H_2)$ and $T_1(D_2)$ and permit some simple conclusions about the nature of the sites for the rapidly relaxing molecular hydrogen components in a-Si:H,D.

In an earlier work Fedders reported[2] calculations of nuclear-spin-lattice relaxation times for protons in dilute $J=1$ o-H_2 (and for deuterons in $J=1$ p-D_2) molecules in a nonmagnetic solid host. These results were applied[3] to the study of dilute o-H_2 in rare-gas solids. There the o-H_2 sites were found to be characterized by large static EFG with "no symmetry." For dilute o-H_2 in solid p-H_2 the static EFG had axial symmetry. Several recent publications[4-7] have employed the $J=1$ theory to analyze the relaxation of H (and D) in amorphous silicon. The H (D) relaxation in plasma-deposited a-Si often displays T_1 minima near 30 K which are associated with rapid spin diffusion of the H (D) magnetization to effectively dilute o-H_2 (p-D_2) relaxation centers. The H_2 (D_2) can act as relaxation centers because their nuclear relaxation times are short (a few milliseconds near 30 K), since the intramolecular-internuclear separation is very small (0.7 Å).

The cold-sample NMR relaxation analyses have determined concentrations of the fast-relaxing molecular H_2 (D_2) relaxation centers to be 100 to 1000 ppm for typical a-Si:H (a-Si:D) samples deposited on substrates at ≤ 330 °C. These analyses have not, however, provided information about the local EFG symmetry or binding configuration for the H_2 (D_2). Recently reported calorimetric (Refs. 8 and 9), ir (Ref. 10), and NMR (Ref. 11) measurements on specially prepared a-Si:H samples have indicated the presence of larger amounts of H_2 (0.5 at.% to a few atomic percent). Fedders *et al.*[12] have pointed out that there must be at least several molecular hydrogen species in a-Si, since the high concentration[8-11] H_2 cannot be the effectively dilute o-H_2 nuclear relaxation centers responsible for H relaxation. For these o-H_2 the electric quadrupole-quadrupole (EQQ) interaction is quenched by proximity to Si void surfaces.

In a-Si there are often significant non-H_2- (non-D_2-) related ($T_{1\beta}$) nuclear relaxation contributions near 300 K. However, there are some published warm-sample H and D relaxation data in a-Si samples where the T_1 does not appear to be dominated by $T_{1\beta}$. It now is of interest to reexamine some of these data and apply the new $J > 1$ theoretical results in an attempt to draw some conclusions about the locations of the fast-relaxing effectively dilute H_2 (D_2) in the a-Si microvoids. If the molecules are adsorbed on internal surfaces, one would expect large static EFG (Ref. 12) with axial, or lower, symmetry. For those H_2 (D_2) trapped as a high-density bulk fluid[11] in void volumes, one would expect[12] smaller EFG and intrinsic relaxation times much less dependent on temperature.

Figure 1 shows 42.3-MHz proton $T_1(H)$ data reported by Carlos *et al.*[6,13,14] for two a-Si:H samples. The data were obtained in the same NMR apparatus, with the same thermometry, etc. Sample "RCA No. 1" was plasma deposited in a dc discharge from 100% SiH_4 (0.5 Torr) at about 300 Å/min onto a 330 °C substrate. It had an electron spin density of 5×10^{15} cm^{-3}. The total H content was determined to be 12 at.%. Some of the RCA No. 1 $T_1(H)$ data points in Fig. 1 have been averaged for the sake of clarity. RCA No. 1 was the sample which was used subsequently in the reported[15] NMR $T_1(H)$ ortho-para conversion studies.

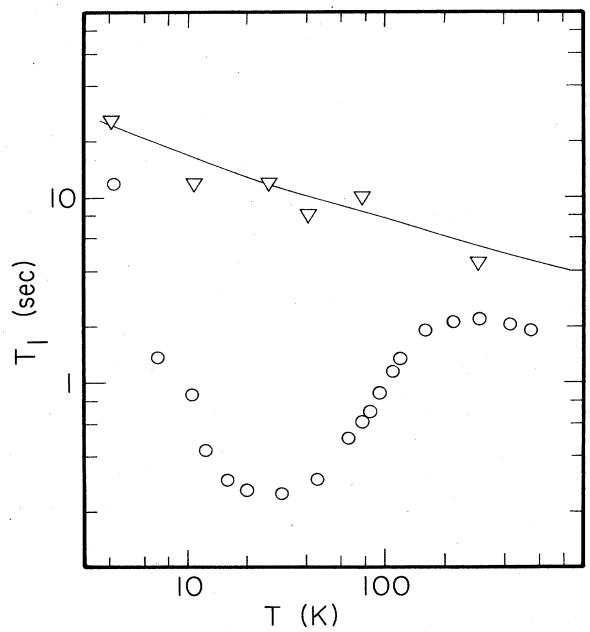

FIG. 1. 42.3 MHz proton spin-lattice relaxation times in two a-Si:H samples reported (Refs. 6, 13, and 14) by Carlos and Taylor. The triangles indicate $T_1(H)$ for a relatively H_2-free sample, Harvard No. 1. The circles indicate $T_1(H)$ for RCA No. 1.

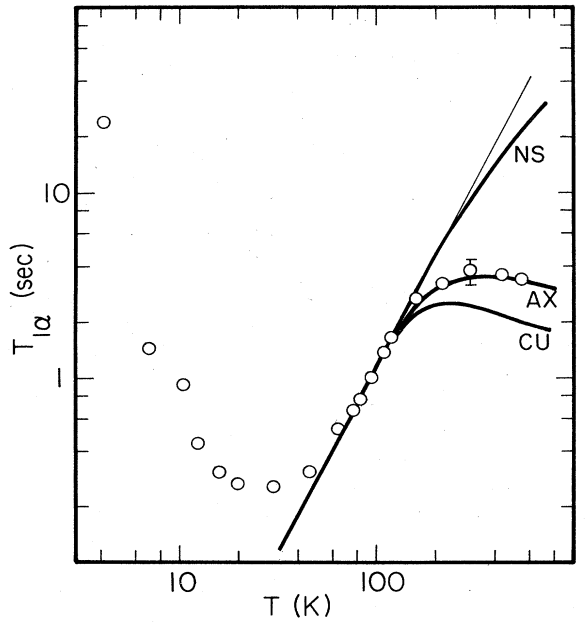

FIG. 2. The H_2-related component of the proton relaxation $T_{1\alpha}(H)$ in sample RCA No. 1 is compared with the temperature dependences predicted for relaxation by rapid spin diffusion to effectively dilute molecular o-H_2 in sites with large static electric-field gradients of no symmetry, axial symmetry, and cubic symmetry. The straight line indicates the T^2 temperature dependence associated with relaxation to $J=1$ molecules only.

The second sample for which $T_1(H)$ data are shown (triangles) in Fig. 1 is Harvard No. 1, which was a sputtered a-Si:H sample specially prepared[14] to have little or no H_2. The solid line indicates the temperature variation of $T_1(H)$ for this H_2-free sample and is typical of the temperature variation of $T_{1\beta}(H)$ usually interpreted as arising from proton relaxation via electronic dangling bonds in the a-Si.

If we write[5]

$$\frac{1}{T_1(H)}=\frac{1}{T_{1\beta}(H)}+\frac{1}{T_{1\alpha}(H)}\ , \tag{1}$$

where $T_{1\alpha}(H)$ is the H_2-related component of the proton relaxation, and take the line through the Harvard No. 1 data to represent a reasonable approximation to $T_{1\beta}(H)$, then the resulting RCA No. 1 $T_{1\alpha}(H)$ are shown as circles in Fig. 2. RCA No. 1 had a larger dangling bond electron spin density[6,14] than did Harvard No. 1 and it may be that the $T_{1\alpha}(H)$ data have been overcorrected for non-H_2-related relaxation. However, in Fig. 2 the total $T_{1\beta}(H)$ correction shifts the warm-sample data by less than a factor of 2 and the conclusions which follow are not affected by the precise selection of $T_{1\beta}(H)$.

The sloping straight line in Fig. 2 indicates a T^2 dependence normalized to the $T_{1\alpha}(H)$ data between 70 and 120 K. It was the observation of this T^2 dependence which first lead to the conclusion[4] that phonon-scattering relaxation of molecular H_2 was responsible for the $T_1(H)$ minimum in RCA No. 1.

The three curved lines in Fig. 2 are normalized to the same T^2 region of the $T_{1\alpha}(H)$ data and indicate the calcu-

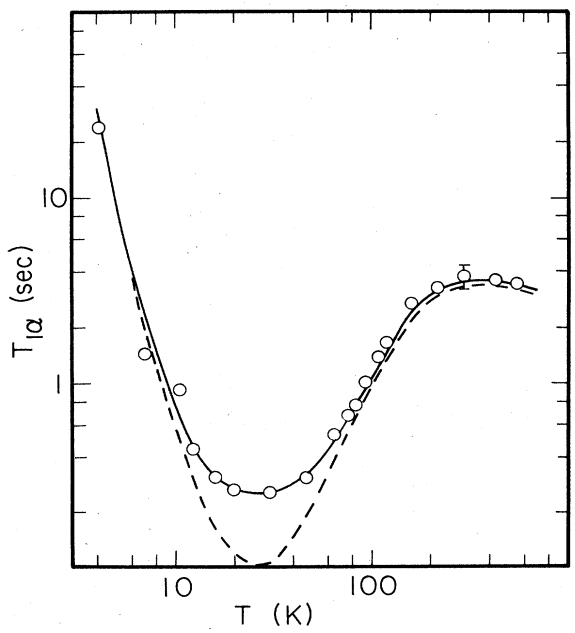

FIG. 3. $T_{1\alpha}(H)$ for sample RCA No. 1 are fitted to relaxation via effectively dilute o-H_2 located in EFG of axial symmetry. The solid line includes relaxation below 100 K according to the expression $T_1(H)=150T_1(H_2)+0.16$ sec. The dashed line indicates the calculated relaxation without the 0.16-sec bottleneck term.

lated[1] temperature variations of $T_1(H_2)$ including $J>1$ states, and for large static EFG of no symmetry, axial symmetry, and cubic symmetry (i.e., no EFG). The cubic and no-symmetry lines indicate the limiting possible temperature dependences for $T_1(H_2)$ in the presence of large static EFG of any symmetry. It is clear that the axial EFG configuration provides a convincing approximation of the warm-sample $T_{1\alpha}(H)$ relaxation in RCA No. 1 from 80 to 550 K. This conclusion is quite insensitive to the precise choice of a $T_{1\beta}(T)$ term. In the ortho-para conversion experiments,[15] the warm-sample $T_1(H)$ data (≥ 300 K) increased with time,[16] so a significant fraction of that relaxation is known to reflect an H_2-related $T_{1\alpha}(H)$.

The proton $T_{1\alpha}(H)$ minima in plasma-deposited a-Si:H samples have been fitted[4-7] with a combination of rapid spin-diffusion and spin-diffusion bottleneck terms:

$$T_{1\alpha}(H)=AT_1(H_2)+B\ . \tag{2}$$

The RCA No. 1 $T_{1\alpha}(H)$ data of Fig. 2 are shown again in Fig. 3. The solid line in Fig. 3 shows Eq. (2) fitted over the full range of the data. Above 100 K the dashed line in Fig. 3 is just the axial-symmetry line of Fig. 2, displaced downward slightly to accommodate a bottleneck term[4] $B=0.16$ sec. The rest of the dashed curve below 100 K represents $AT_1(H_2)$ with $A=150$ and $T_1(H_2)$ calculated[2,3] for relaxation in effectively dilute $J=1$ o-H_2 with a 42.3-MHz Larmor frequency, large static EFG of axial symmetry, a $T_{1\alpha}(H)$ minimum at 26 K, and a characteristic temperature $\Theta_c=40$ K for the phonon dynamics[17,18] which govern the molecular relaxation rate Γ_2. For $n(H)=12$ at. %, the determined spin heat-capacity ratio A corresponds to $n(H_2)=1.7\times10^{19}$ cm^{-3} or 340 ppm.

The need for a bottleneck term is evident in Fig. 3 and the addition of $B=0.16$ sec [Eq. (2)] brings the dashed line up to the solid line in Fig. 3, in excellent agreement with all the $T_{1\alpha}(H)$ data. It is noteworthy that the calculated $T_{1\alpha}(H)$ line passes close to the long relaxation-time data point at 4.2 K. This will be shown to mean that in sample I the EQQ interaction was very small ($<10^6$ sec^{-1}) between those o-H_2 molecules responsible for the $T_{1\alpha}(H)$ proton relaxation.

Figure 4 shows the results of a calculation[2,3] of $\Gamma_2(T)$ corresponding to each $T_{1\alpha}(H)$ data point below 120 K in Fig. 3. Θ_c does not enter into the calculation. The resulting $\Gamma_2(T)$ data range over most of the complete anticipated phonon-relaxation spectrum of temperature dependences of Γ_2, from T^2 near 100 K to T^7 at low temperatures. Any small EQQ-related rate Γ_Q would appear here as a constant temperature-independent Γ_Q term at the lower-left corner of Fig. 4. Clearly $\Gamma_Q<10^6$ sec^{-1} for this a-Si:H sample. Γ_Q for solid normal H_2 (Refs. 12 and 19) is $\simeq10^{12}$ sec^{-1}. Fedders *et al.*[12] have pointed out that such a reduction of EQQ and Γ_Q can result either from great diluation of the o-H_2 molecules (which would not fit the o-p conversion results), or from large static EFG (much larger than EQQ), which vary significantly from one o-H_2 site to the next adjacent o-H_2 site, probably for o-H_2 adsorbed on submicroscopically rough internal surfaces.

Our previous analysis[4] of the RCA No. 1 $T_1(H)$ data

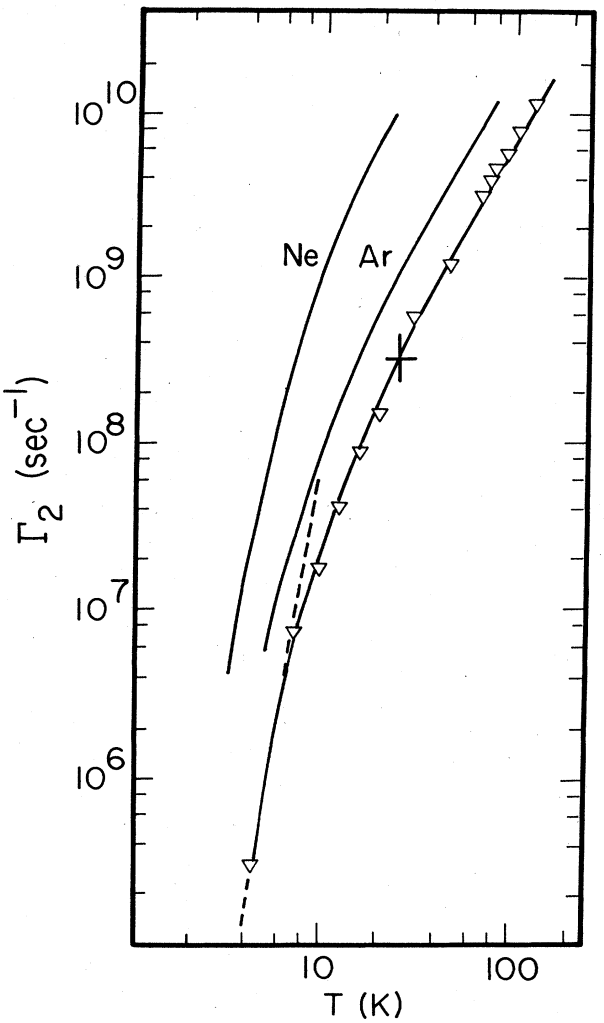

FIG. 4. The triangles indicate molecular o-H_2 correlation rates Γ_2 calculated from the $T_{1\alpha}(H)$ data of Figs. 2 and 3. A cross indicates the location of the $T_{1\alpha}(H)$ minimum. For comparison two solid curves at the left indicate $\Gamma_2(T)$ reported (Ref. 3) for dilute o-H_2 in solid neon and argon. The dashed line indicates a limiting T^7 temperature dependence at low temperatures.

used the $J=1$ calculations to fit only the cold-sample $T_1(H)$ minimum. The static EFG were taken to have no symmetry and the $n(H_2)$ deduced from the rapid spin-diffusion term in Eq. (2) differed by a factor of 2 from the 1.7×10^{19} cm^{-3} determined above. However, the $n(H_2)$ deduced from the 0.16 sec bottleneck term was 1.7×10^{19} cm^{-3}, in agreement with the present axial-symmetry result for the rapid spin-diffusion term.

Uncorrected proton times $T_1(H)$ are shown in Figs. 5 and 6 for a quite different category of a-Si:H samples. Sample III was prepared at Xerox Palo Alto Research Center (PARC) by rf deposition at 0.1 W/cm^2 from SiH_4 gas onto an electrically grounded substrate heated to 230 °C. A NMR spin count showed[7,20] the sample to contain 10.9 at. % H. In Fig. 5 the T^2 line and the three curved lines have the same significance as in Fig. 2. They have been normalized to correspond to $J=1$ and the

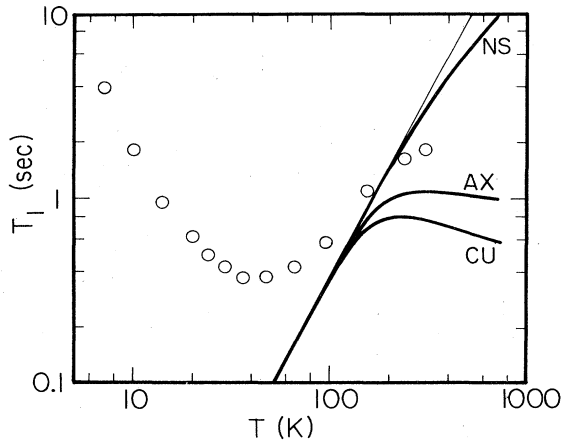

FIG. 5. Proton relaxation times T_1(H) at 91.8 MHz in sample III (Xerox). The light line indicates a T^2 variation. The heavy curved lines indicate temperature dependences for relaxation to molecular o-H_2 in sites with EFG of no symmetry, axial symmetry, and cubic symmetry. Even without $T_{1\beta}$ corrections the relaxation data can be fitted only by the case of EFG of low symmetry.

determined[7,20] bottleneck $B=0.22$ sec for the data between 66 and 156 K. Sample Xerox No. 39 was prepared[21] at Xerox PARC in a large area ($\simeq$600 cm^2) deposition chamber at 0.025 W/cm^2 from SiH_4 gas onto a 230°C substrate and had a thickness of 1 μm. The sample had 12.7 at.% H. Even without any $T_{1\beta}$(H) correction, the raw T_1(H) data of Figs. 5 and 6 clearly cannot reflect relaxation by H_2 located in EFG of axial, or higher, symmetry. At 300 K those $J>1$ calculated relaxations have leveled off or begun to decrease with increasing temperature. On the other hand, the T_1(H) data still are increasing with temperature at 300 K and can be fitted only for relaxation to o-H_2 situated in EFG with lower than axial symmetry. A reasonable $T_{1\beta}$(H) curve, parallel to that in Fig. 1, and the assumption of EFG of

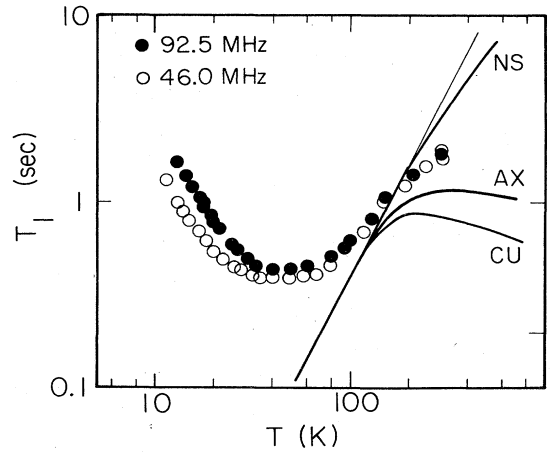

FIG. 6. Proton relaxation times T_1(H) at 92.5 and 46 MHz in Xerox PARC Sample No. 39. As in Fig. 5 the data can be fitted only for relaxation by effectively dilute o-H_2 located in EFG of low symmetry.

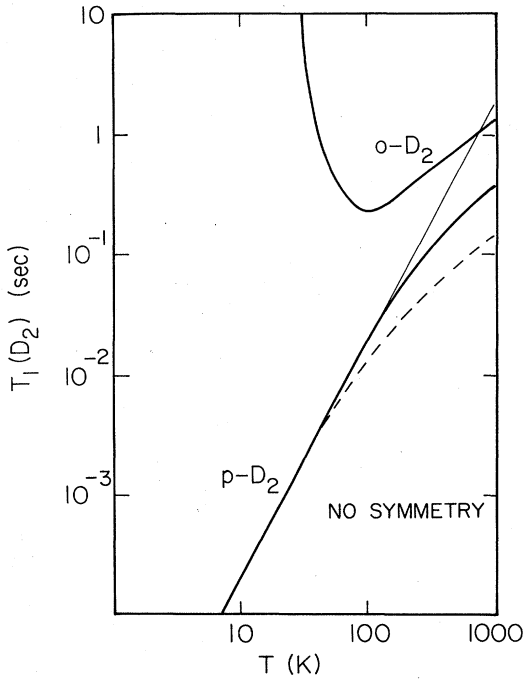

FIG. 7. Fedders' calculated[1] deuteron nuclear-spin-lattice relaxation times for dilute o-D_2 and p-D_2 located in large static EFG of no symmetry in solid nonmagnetic hosts. The relaxation times are calculated for an interaction strength of 10^5 sec^{-1}K^{-2}. The light straight line indicates the T^2 behavior expected for $J=1$. The curved dashed line indicates the anticipated composite relaxation by o-D_2 and p-D_2, normalized to the T^2 line.

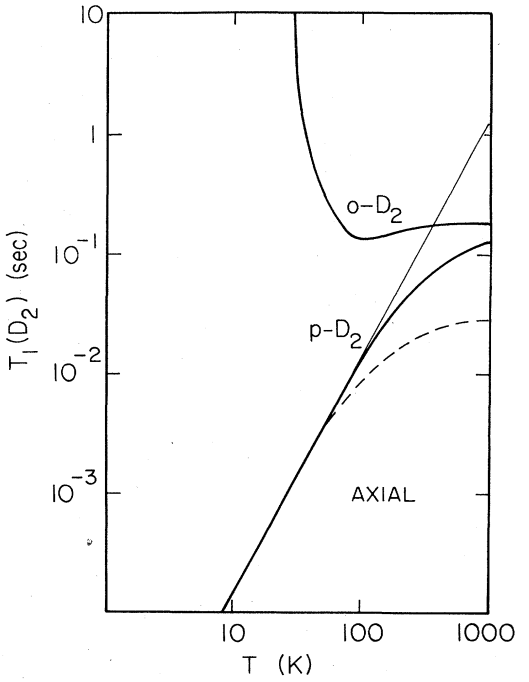

FIG. 8. Calculated deuteron nuclear relaxation times for dilute o-D_2 and p-D_2 as in Fig. 7, but located in large static EFG of axial symmetry.

no symmetry provides an excellent fit to the limited $T_1(H)$ data of Figs. 5 and 6. Although proton relaxation measurements were made only up to 300 K, the results nevertheless exclude the possibility of EFG of axial (or higher) symmetry at the o-H_2 relaxation centers. Thus, comparison of RCA No. 1 and of Xerox III and Xerox No. 39 shows that there are at least two different types of relaxation-center o-H_2 sites in a-Si:H. In none of the more than ten a-Si samples thus far analyzed does anything approaching the $T_1(H_2)$ temperature dependence corresponding to cubic symmetry occur. The samples III and No. 39 type of $T_1(H)$ temperature dependence are characteristic of most of the current NMR results for good-quality nonannealed samples plasma deposited on warm substrates ($\lesssim 300$ °C).

The calculated[1] results for the warm ($J>1$)-dominated $T_1(D_2)$ relaxation times for dilute molecular D_2 yield the temperature dependences shown by the solid lines in Figs. 7, 8, and 9 for the cases no symmetry, axial symmetry, and cubic symmetry. The lines are calculated for a typical[1] interaction strength, 10^5 $\sec^{-1}K^{-2}$. The light straight lines indicate a T^2 temperature variation. The axial and cubic curves ultimately turn over and come to horizontal lines for temperatures $\gtrsim 10^4$ K. The peak $T_1(D_2)$ values occur at temperatures larger than 1000 K.

The curved dashed lines indicate (normalized to the T^2 lines) the composite temperature dependences anticipated for deuteron $T_{1\alpha}(D)$ in a-Si:D in the case of rapid spin diffusion to both p-D_2 and o-D_2 relaxation centers, assumed to be present randomly in thermal equilibrium populations.

The relaxing fraction of o-D_2 has $I=2$ and a relative population of $\frac{5}{9}$. The p-D_2 molecules have $I=1$ and a relative population of $\frac{3}{9}$. Their relative weights as relaxation centers are given by the spin heat-capacity ratio of the quantity $(2I+1)I(I+1)$ which is 5:1 for o-D_2:p-D_2. For rapid spin diffusion the $T_1(D)$ should reflect a composite $T_1(D_2)$ given by the weighted averages of the o-D_2 and p-D_2 relaxation rates. These are indicated by the dashed lines, which have been displaced down by a factor of 5 to correspond to the indicated T^2 lines. The o-D_2 contributions rapidly become important as soon as the temperature is high enough to appreciably populate the $J=2$ state.

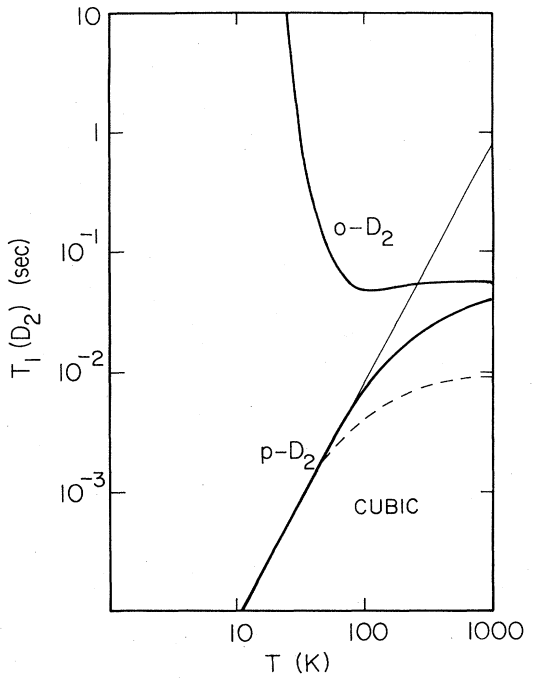

FIG. 9. Calculated deuteron nuclear relaxation times for dilute o-D_2 and p-D_2 as in Fig. 7, but located in EFG of cubic symmetry (i.e., no EFG).

Unfortunately this wealth of predicted warm-sample $T_1(D_2)$ relaxation behavior is difficult to investigate experimentally because signal-to-noise limitations make deuteron magnetic resonance (DMR) relaxation measurements above room temperature a tedious task. Hardy has reported[22,23] some $T_1(D_2)$ measurements below 330 K in D_2 gas which follow the general character of the o-D_2 and p-D_2 lines in Fig. 9.

There are reported[5,24] $T_1(D)$ data to 300 K at 14.4 and 30.0 MHz in an a-Si:D,H sample. This material, "Sample I," was rf plasma deposited at ~ 1 W/cm^2 onto a room-temperature ungrounded substrate. The starting gas mixture was 5% SiH_4, 95% D_2 and the sample contained 7 at. % H and 24 at. % D. The Fourier-transform DMR (FTDMR) quadrupole echo line-shape spectra are shown in Fig. 10 for sample I at 4.2 and 39 K. There is a sharply defined $\eta=0$ quadrupolar Pake doublet associated[5,20] with the silicon-deuteron bond coupling strength. This component shows a long $T_1(D)$ (hundreds of seconds) with a temperature dependence characteristic of a dangling-bond-determined $T_{1\beta}(D)$. There also is an unresolved quadrupole-broadened central line with a motionally averaged temperature-dependent linewidth and a clear D_2-related T_1 minimum. These latter central-component relaxation data at 14.4 and 30 MHz are shown in Fig. 11.

The straight line in Fig. 11 shows a T^2 $J=1$ temperature dependence normalized to a bottleneck of 0.13 sec and to the 14.4 MHz data between 44 and 100 K. The curved lines indicate (with the same normalization) the predicted temperature dependences of the composite (o-D_2+p-D_2) dashed lines of Figs. 7, 8, and 9. None of the three curved lines fit the data very well. The observed relaxation times between 77 and 170 K are significantly larger than can be accounted for by the composite relaxation curves for any symmetry of static EFG. Obviously no additional $T_{1\beta}(D)$ process can account for the fact that the T_1 data of Fig. 11 are larger in this temperature interval than can arise from the temperature dependences associated with relaxation to molecular D_2 relaxation centers in the a-Si. It is evident that the 14.4 MHz T_1 results instead exhibit a T^2 dependence of over a full factor of 10 in relaxation times and up to a temperature of 120 K. For relaxation via effectively dilute molecular D_2 significant deviation from T^2 is expected to begin between 40 and 80 K, depending on the symmetry of the EFG.

Clearly something limits the relaxation via D_2 above 40 K. A probable candidate is motional narrowing. The T_1 data of Fig. 11 are associated with the motionally narrowed central component of the DMR line. RCA No. 1 is

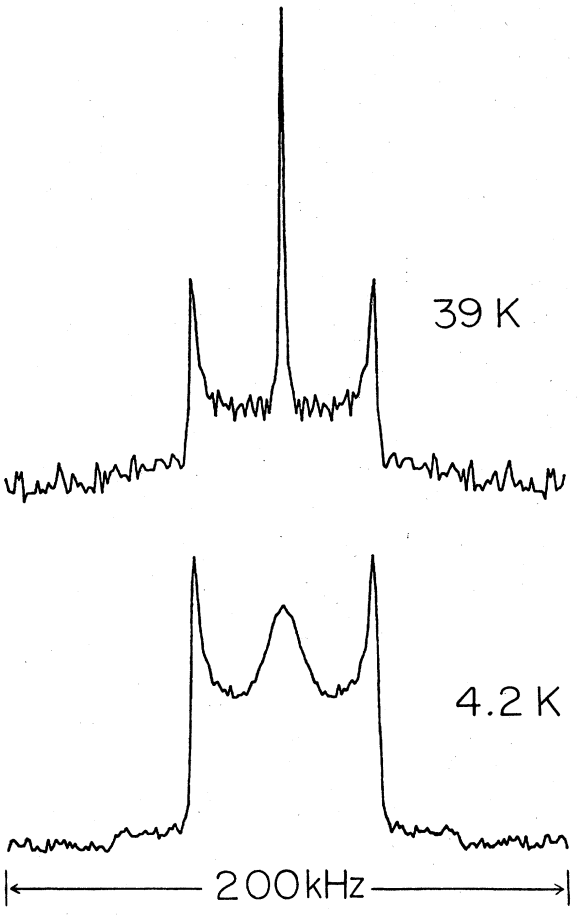

FIG. 10. FTDMR quadrupole echo line-shape spectra for sample I at 4.2 and 39 K. The resolved doublet splitting is 66±1 kHz.

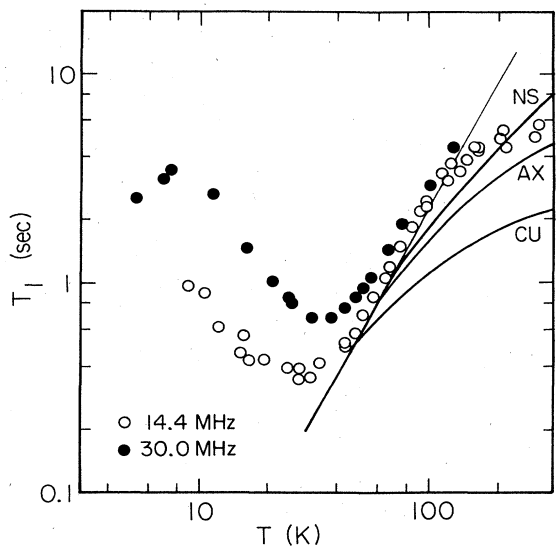

FIG. 11. Deuteron spin-lattice relaxation times at 14.4 and 30 MHz for the narrowed central component of the sample I resonances shown in Fig. 10. The light line shows T^2 and the dark curves the composite relaxations from the dashed curves of Figs. 7—9, normalized to the T^2 line.

anomalous among the a-Si:D,H samples we have studied[20] in that it has a large motionally narrowed central DMR line-shape fraction. In most samples this component is numerically insignificant and the DMR consists principally of the resolved doublet and a broad central line. Both the resolved doublet and the broad central line have quadrupolar widths near 66 kHz full width at half maximum (FWHM). This also provides a reasonable magnitude for the rigid-lattice quadrupolar width of the narrow central component. Measurements of the quadrupole echo damping rate at 4 K indicate[5] that the narrow central component has a deuteron-deuteron dipolar interaction strength of 1.5 $\text{msec}^{-1}=670$ Hz. Therefore, in the rigid-lattice regime the ratio of quadrupolar-to-dipolar widths in sample I is 10^2.

However, in the motionally well-narrowed regime these widths are reduced to

$$\delta\nu_q=\nu_q^2/\nu_c \tag{3}$$

and

$$\delta\nu_d=\nu_d^2/\nu_c\ , \tag{4}$$

and the ratio $\delta\nu_q/\delta\nu_d$ becomes 10^4. For temperatures warm enough that ν_c is significantly larger than 66 kHz, the dipolar rates become much smaller than the residual quadrupolar broadening. It is probable that the deuteron spin-diffusion process becomes significantly less effective in the narrow component above 40 K and T_1(D) increases until a non-D_2-related $T_{1\beta}$ process becomes important near 150 K.

CONCLUSIONS

The results of Carlos and Taylor[6,13,14] for proton relaxation times in a-Si:H RCA No. 1 are in excellent agreement with the $J>1$ calculations[1] and relaxation by effectively dilute o-H_2 molecules located at sites with large static EFG of axial symmetry. The intermolecular EQQ interaction among these o-H_2 is reduced by a factor of 10^6 from that[12,19] for solid normal hydrogen. Other samples more recently prepared at Xerox PARCS show proton relaxation by o-H_2 molecules located in EFG of symmetry lower than axial and perhaps of no symmetry. Since the o-H_2 relaxation centers have been demonstrated[12] to be located near the surfaces of microvoids in the a-Si, the deduced EFG symmetries distinguish categories of physisorption sites for the H_2. A reasonable conclusion is that the axial-symmetry EFG are associated with H_2 in small voids ~ 5 Å in diameter and the low-symmetry EFG characterize H_2 adsorbed on microscopically rough surfaces, including those of larger voids. A similar conclusion concerning the small voids was drawn by Carlos and Taylor,[6] based on the high-temperature annealing behavior of the H_2 in RCA No. 1.

The limited deuteron relaxation data are insufficient to permit general conclusions about the D_2 relaxation centers. The data are better fitted by relaxation to p-D_2 and o-D_2 in sites with EFG of no symmetry rather than axial or higher symmetry. However, even in the no-symmetry case, it is necessary to invoke motional narrowing of the central DMR component in order to fit the temperature dependence of $T_1(D)$.

ACKNOWLEDGMENTS

This work was supported in part by the National Science Foundation (Low Temperature Physics Program) under Grant No. DMR-82-04166. The author would like to acknowledge many useful discussions with Peter A. Fedders and Ron Fisch. J. B. Boyce, W. E. Carlos, D. J. Leopold, and P. C. Taylor kindly provided tabulations of experimental data.

[1]P. A. Fedders, Phys. Rev. B **30**, 3603 (1984).
[2]P. A. Fedders, Phys. Rev. B **20**, 2588 (1979).
[3]M. S. Conradi, K. Luszczynski, and R. E. Norberg, Phys. Rev. B **20**, 2594 (1979).
[4]M. S. Conradi and R. E. Norberg, Phys. Rev. B **24**, 2285 (1981).
[5]D. J. Leopold, J. B. Boyce, P. A. Fedders, and R. E. Norberg, Phys. Rev. B **26**, 605 (1982).
[6]W. E. Carlos and P. C. Taylor, Phys. Rev. B **26**, 3605 (1982).
[7]D. J. Leopold, B. S. Coughlan, P. A. Fedders, R. E. Norberg, J. B. Boyce, and J. C. Knights, J. Non-Cryst. Solids **66**, 121 (1984).
[8]H. v. Löhneysen, H. J. Schink, and W. Beyer, Phys. Rev. Lett. **52**, 549 (1984); J. E. Graebner, B. Golding, L. C. Allen, D. K. Biegelsen, and M. Stutzmann, *ibid.* **52**, 553 (1984).
[9]J. E. Graebner, L. C. Allen, and B. Golding, Phys. Rev. B **31**, 904 (1985).
[10]Y. J. Chabal and C. K. N. Patel, Phys. Rev. Lett. **53**, 210 (1984); **53**, 1771 (1984).
[11]B. Lamotte, Phys. Rev. Lett. **53**, 576 (1984); J. B. Boyce and M. Stutzmann, *ibid.* **54**, 562 (1985).
[12]P. A. Fedders, R. Fisch, and R. E. Norberg, Phys. Rev. B (to be published).
[13]W. E. Carlos and P. C. Taylor, Phys. Rev. Lett. **45**, 358 (1980).
[14]W. E. Carlos, P. C. Taylor, S. Oguz, and W. Paul, in *Tetrahedrally Bonded Amorphous Semiconductors,* Topical Conference on Tetrahedrally Bonded Amorphous Semiconductors, Carefree, Arizona, edited by R. A. Street, D. K. Biegelsen, and J. C. Knights (AIP, New York, 1981), p. 67.
[15]W. E. Carlos and P. C. Taylor, Phys. Rev. B **25**, 1435 (1982).
[16]P. C. Taylor (private communication).
[17]J. Van Kranendonk, Physica (Utrecht) **20**, 871 (1954).
[18]J. Van Kranendonk and M. B. Walker, Can. J. Phys. **46**, 2441 (1968).
[19]C. W. Myles and C. Ebner, Phys. Rev. B **11**, 2339 (1975); **12**, 1608(E) (1975).
[20]D. J. Leopold, P. A. Fedders, R. E. Norberg, J. B. Boyce, and J. C. Knights, Phys. Rev. B (to be published).
[21]J. B. Boyce and M. J. Thompson, J. Non-Cryst. Solids **66**, 127 (1984).
[22]W. N. Hardy, Ph.D. thesis, University of British Columbia, 1961 (unpublished).
[23]M. Bloom, I. Oppenheim, M. Lipsicas, C. G. Wade, and C. F. Yarnell, J. Chem. Phys. **43**, 1036 (1965).
[24]D. J. Leopold, Ph.D. thesis, Washington University, 1983 (unpublished).